Monthly Notices
of the
ROYAL ASTRONOMICAL SOCIETY

MNRAS **429,** 2934–2944 (2013) doi:10.1093/mnras/sts522

Magnetic white dwarf stars in the Sloan Digital Sky Survey

S. O. Kepler,[1]★ I. Pelisoli,[1] S. Jordan,[2] S. J. Kleinman,[3] D. Koester,[4] B. Külebi,[5,6] V. Peçanha,[1] B. G. Castanheira,[7,8] A. Nitta,[3] J. E. S. Costa,[1] D. E. Winget,[8] A. Kanaan[9] and L. Fraga[10]

[1]*Instituto de Física, Universidade Federal do Rio Grande do Sul, 91501-900 Porto-Alegre, RS, Brazil*
[2]*Astronomisches Rechen-Institut, Zentrum für Astronomie der Universität Heidelberg, Mönchhofstr. 12-14, D-69120 Heidelberg, Germany*
[3]*Gemini Observatory, Hilo, HI 96720, USA*
[4]*Institut für Theoretische Physik und Astrophysik, Universität Kiel, D-24098 Kiel, Germany*
[5]*Institut de Ciències de L'Espai, Universitat Autònoma de Barcelona, Barcelona, Spain*
[6]*Institute for Space Studies of Catalonia, c/Gran Capità 2-4, Edif. Nexus 104, E-08034 Barcelona, Spain*
[7] *Institut für Astronomie, Wien, Austria*
[8]*McDonald Observatory and Department of Astronomy, University of Texas, Austin, TX 78712, USA*
[9] *Universidade Federal de Santa Catarina, Florianópolis, SC, Brazil*
[10] *Soar Telescope, La Serena, Chile*

Accepted 2012 November 30. Received 2012 November 24; in original form 2012 April 7

ABSTRACT

To obtain better statistics on the occurrence of magnetism among white dwarfs, we searched the spectra of the hydrogen atmosphere white dwarf stars (DAs) in the Data Release 7 of the Sloan Digital Sky Survey (SDSS) for Zeeman splittings and estimated the magnetic fields. We found 521 DAs with detectable Zeeman splittings, with fields in the range from around 1 to 733 MG, which amounts to 4 per cent of all DAs observed. As the SDSS spectra have low signal-to-noise ratios, we carefully investigated by simulations with theoretical spectra how reliable our detection of magnetic field was.

Key words: stars: magnetic field – white dwarfs.

1 INTRODUCTION

In the latest white dwarf catalogue based on the Sloan Digital Sky Survey (SDSS) Data Release 7 (DR7), Kleinman et al. (2013) classify the spectra of 19 713 white dwarf stars, including 12 831 hydrogen atmosphere white dwarf stars (DAs) and 922 helium atmosphere white dwarf stars (DBs). The authors fit the optical spectra from 3900 to 6800 Å to DA and DB grids of synthetic non-magnetic spectra derived from model atmospheres (Koester 2010). The SDSS spectra have a mean g-band signal-to-noise ratio S/N(g) $\approx$ 13 for all DAs and $\approx$21 for those brighter than $g = 19$.

Through visual inspection of all these spectra, we identified Zeeman splittings in the spectra of 521 DA white dwarfs, 11 with multiple spectra. The main objective of this paper is to identify these stars and estimate their magnetic field. Independently, Külebi et al. (2009) found 44 new magnetic white dwarfs in the same SDSS DR7 sample, and used $\log g = 8.0$ models to estimate the fields of the 141 then known magnetic white dwarfs, finding fields from $B = 1$ to 733 MG. We report here on the estimate of the Zeeman splittings in $\simeq$4 per cent of all DA white dwarf stars. With the low resolution ($R \simeq 2000$) of the SDSS spectra, magnetic fields weaker than 2 MG are only detectable for the highest S/N spectra (e.g. Tout et al. 2008). We first summarize some previous results on magnetic white dwarfs.

2 MAGNETIC WHITE DWARFS AND THEIR PROGENITORS

The magnetic nature of the until then unexplained spectra of the white dwarf GRW+70.8247 was confirmed by Kemp (1970). His magneto-emission model, which predicted the level of continuum polarization, was not quite adequate for the high magnetic field in this star, and the estimated field strength of 10 MG later turned out to be much too low, but the general idea that the strange spectrum was caused by a magnetic field was correct. The detailed description of the spectra became possible only with extensive calculations of the atomic transitions of hydrogen developed by Roesner et al. (1984) and Greenstein, Henry & O'Connell (1985), and a consistent atmospheric modelling by Wickramasinghe & Ferrario (1988) and Jordan (1992).

The number of known magnetic white dwarfs has increased significantly since the first identifications. Liebert, Bergeron & Holberg (2003) found that only 2 per cent of the 341 DAs and 15 DBs in the Palomar–Green Survey were magnetic, that is, exhibited Zeeman splitted lines. However, they estimated that up to 10 per cent could be magnetic, if the magnetic white dwarfs are more massive than average white dwarfs and therefore had smaller radius and

★ E-mail: kepler@if.ufrgs.br

luminosities, as indicated by Liebert et al. (1988) and Sion et al. (1988). Kawka et al. (2003) estimated that up to 16 per cent of all white dwarfs may be magnetic. Jordan et. al. (2007), based on spectropolarimetry using the 8.2-m VLT telescope at ESO, estimated that up to 15–20 per cent of all white dwarfs are magnetic at the kilogauss (kG) level. Landstreet et al. (2012) re-analysed the spectropolarimetry with a new state-of-the-art calibration pipeline and added further new observations. From the total sample of 35 DA stars, they found that about 10 per cent (between 2.8 and 30 per cent at the 95 per cent confidence level) were magnetic at the kG level. In the local 20 and 25 pc volume limited samples, there are $\simeq$7 per cent magnetic white dwarfs, according to Giammichele, Bergeron & Dufour (2012) and Holberg, Sion & Oswalt (2011). An accurate estimate of this percentage is crucial for an understanding of the origin of the magnetic fields.

Historically, the explanation of the magnetic fields in white dwarfs has been as fossil fields, motivated by the slow Ohmic decay in degenerate matter (e.g. Braithwaite & Spruit 2004; Tout, Wickramasinghe & Ferrario 2004; Wickramasinghe & Ferrario 2005). From the discovery of kG magnetic fields in the atmospheres of peculiar early-type stars, the Ap and Bp stars, Babcock (1947a,b) already demonstrated that conservation of the magnetic flux during the stellar evolution could lead to field strengths as high as a MG in the white dwarfs resulting from the evolution.

Ap/Bp stars constitute less than 10 per cent of all intermediate-mass main-sequence stars (e.g. Power et al. 2008), and can account for a fraction of 4.3 per cent magnetic white dwarfs, but they should produce white dwarfs with fields above 100 MG (Kawka et al. 2003) if the magnetic flux is fully conserved during the stellar evolution. Wickramasinghe & Ferrario (2005), via population synthesis, conclude that the current number distribution and masses of high-field magnetic white dwarfs ($B > 1$ MG) can be explained if $\approx$40 per cent of main-sequence stars more massive than 4.5 $M_\odot$ have magnetic fields in the range of 10–100 G, which is below the current level of detection.

Schmidt & Smith (1995), Liebert et al. (1988), Sion et al. (1988), Liebert et al. (2003) and Kawka et al. (2007) find that magnetic white dwarfs are more massive than non-magnetic ones by fitting the wings of the spectral lines to theoretical spectra, supposedly unaffected by the magnetic fields. Tout & Regos (1995), Tout et al. (2008) and Nordhaus (2011) propose that white dwarfs with fields above 1 MG are produced by strong binary interactions during the post-main-sequence evolution, while García-Berro et al. (2012) propose that high magnetic field white dwarfs are produced by the merger of two degenerate cores and that the expected number agrees with observations. These proposals are in line with the cited observation that magnetic white dwarf stars have, in general, higher masses than average single white dwarf stars. Kundu & Mukhopadhyay (2012) and Das & Mukhopadhyay (2012) propose that highly magnetic white dwarfs could have limiting masses substantially higher than the Chandrasekhar limit. On the other hand, Wegg & Phinney (2012) conclude that the kinematics of massive white dwarfs are consistent with the majority being formed from single star evolution.

3 DETECTION OF MAGNETIC FIELDS IN SDSS DR7 WHITE DWARFS

We classified more than 48 000 spectra, selected as possible white dwarf stars from the SDSS DR7 by their colours, through visual inspection and detected Zeeman splittings in 521 DA stars. Fig. 1 shows the spectra of one of the newly identified magnetic white dwarfs as an example. As we were able to detect only magnetic fields down to 1–3 MG in strength, because of the $R \simeq 2000$ resolution and relatively low S/N of most spectra ($\langle S/N \rangle \simeq 13$), the 4 per cent detected (521/12 831 DAs) is a lower limit and the actual number of magnetic white dwarf stars should be larger if we include smaller field strengths. The identified magnetic white dwarf stars cover the whole range of temperature and spectral classes observed (Kleinman et al. 2013). Figs 2 and 3 show spectra of a few of the highest S/N new magnetic white dwarfs we identified, showing a broad range of splittings, and hence of magnetic fields.

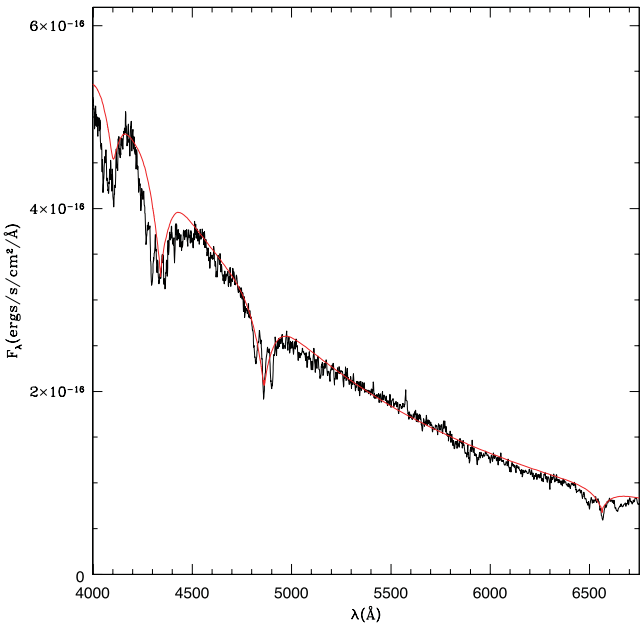

Figure 1. SDSS spectrum of one of the stars we identified for Zeeman splittings, SDSS J111010.50+600141.44, indicative of a 6.2 MG magnetic field. A DA model, *without magnetic field*, of $T_{\rm eff} = 36\,000$ K, $\log g = 9.64$, $M = 1.33$ $M_\odot$ resulting from a least-squares fit to the spectra is plotted in red, obviously inadequate; the lines are wide because of the Zeeman splittings, not due to large pressure (gravity) broadening.

Fig. 4 shows the fraction of detected magnetism in white dwarfs as a function of the S/N provided by Kleinman et al. (2013). The fact that we see an increase of detected magnetic fields in spectra with lower S/N made us suspicious. For this reason, we carefully investigated the influence of the S/N on the detection rate with the help of a blind test using noisy theoretical spectra (see Section 4). Our result was that classification with S/N $\leq$ 10 needs to be confirmed by future observations. Furthermore, any estimate of the overall percentage of magnetic to non-magnetic white dwarf stars needs to take this apparent selection effect into account (Liebert et al. 2003).

3.1 Estimation of the magnetic field strength

For fields stronger than 10 kG but weaker than 2 MG, that is, in the Paschen–Back limit, low-level ($n \leq 4$) lines will be split into three components, with the shifted components separated by around

$$\Delta\lambda = \pm 4.67 \times 10^{-7} \lambda^2 B,$$

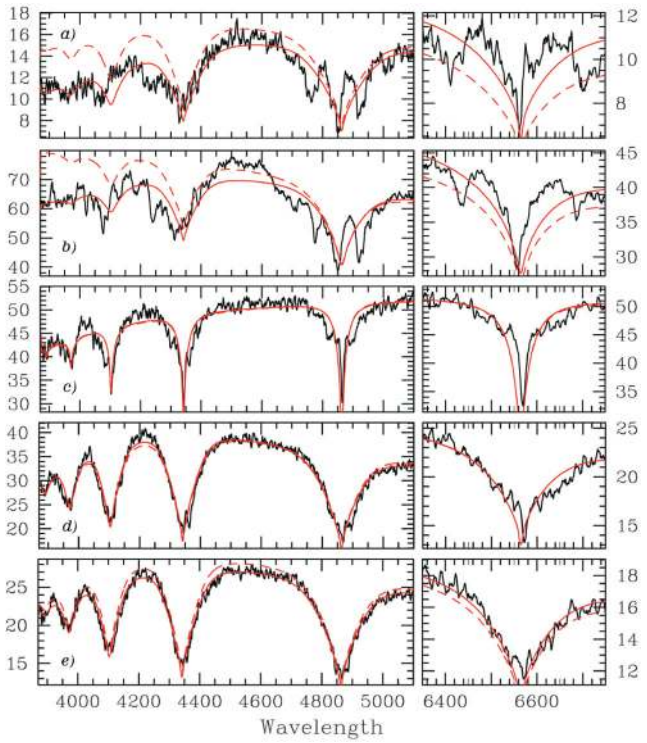

Figure 2. Highest S/N SDSS spectra of a sample of stars for which we identified for Zeeman splittings, indicative of fields from 14 to 1.3 MG. (a) Plate-MJD-Fibre = 1954-53357-393, 13 MG, SDSS J101428.10+365724.40; (b) 0415-51879-378, 11 MG, J033145.69+004517.04; (c) 1616-53169-423, 2.4 MG, 123414.11+124829.58; (d) 2277-53705-484, 2.2 MG, 083945.56+200015.76; (e) 2772-54529-217, 2.2 MG, 141309.30+191832.01; (f) 2694-54199-175, 1.7 MG, 064607.86+280510.14; (g) 2376-53770-534, 2.6 MG, 103532.53+212603.56; (h) 2417-53766-568, 9.9 MG, 031824.20+422651.00; (i) 2585-54097-030, 14 MG, 100759.81+162349.64; (j) 2694-54199-528, 1.3 MG, 065133.34+284423.44; (k) 0810-52672-391, 11 MG, 033145.69+004517.04; (l) 1798-53851-233, 14 MG, 131508.97+093713.87; (m) 2006-53476-332, 19 MG, 125715.54+341439.38; (n) 2644-54210-167, 1.9 MG, 121033.24+221402.64; (o) 2430-53815-229, 2.5 MG, 085106.13+120157.84. DA models, *without magnetic field*, resulting from least-squares fits to the spectra are plotted in red, obviously inadequate.

with λ in Å and B in MG (Jenkins & Segrè 1939; Hamada 1971; Garstang 1977). The quadratic splitting is given by

$$\Delta\lambda_{\rm q} = -\frac{e^2}{a_0^2} 8mc^3h\lambda^2n^4(1+m_\ell^2)B^2$$

$$\simeq -4.97\times10^{-23}\lambda^2n^4(1+m_\ell^2)B^2 \text{ Å},$$

where a_0 is the Bohr radius and m_ℓ is the magnetic quantum number. This formula is valid for 2p $\rightarrow$ ns and 2p $\rightarrow$ nd transitions, where n is the principal quantum number. For the 2s $\rightarrow$ np transitions,

$$\Delta\lambda_{\rm q} \simeq -4.97\times10^{-23}\lambda^2[n^2(n^2-1)(1+m_\ell^2-28)B^2 \text{ Å}.$$

Note that because of the n^4 dependency of the quadratic Zeeman splitting, even for fields around 1 MG, the $n \geq 7$ lines show dominant quadratic splittings (Fig. 5).

For magnetic fields less than $\simeq$2 MG, the Zeeman splitting is difficult to observe in low-resolution spectra of white dwarfs because the spectral lines are already broadened due to the high density.

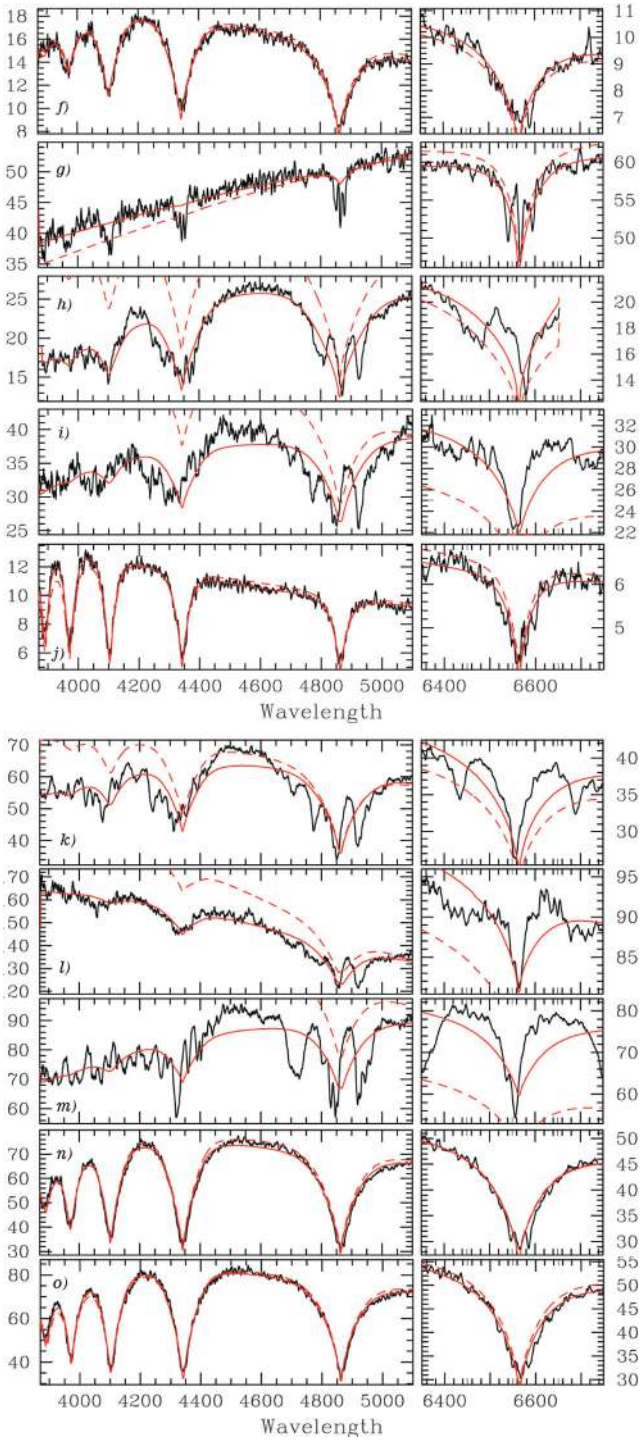

Figure 2 – *continued*

The linear Zeeman splitting is equivalent to a broadening of unpolarized spectral lines of the order of 10 km s^{-1} for fields around 10 kG. For higher fields, the magnetic energy cannot be included as a perturbation because the cylindrical symmetry of the magnetic field starts to disturb the spherical symmetry of the Coulomb force that keeps the hydrogen atoms together. For the $n = 1$ level, the Lorentz force and the Coulomb force are of the same order for $B = 4670$ MG. As the energy of the levels is proportional to the inverse of n^2, the higher levels are disturbed for much smaller fields.

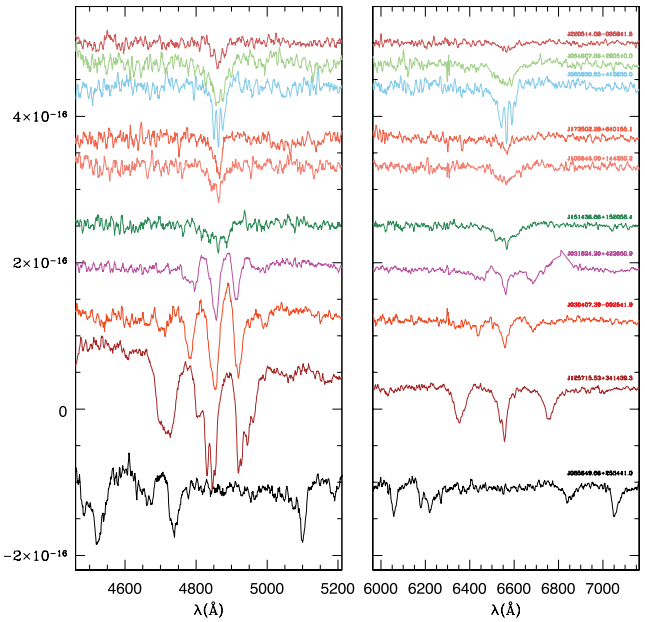

Figure 3. Hβ (left-hand panel) and Hα (right-hand panel) line profiles for a sample of new magnetic white dwarf stars, with fields of $\simeq$3 MG at the top and 90 MG at the bottom. The y-axis shows flux in arbitrary units.

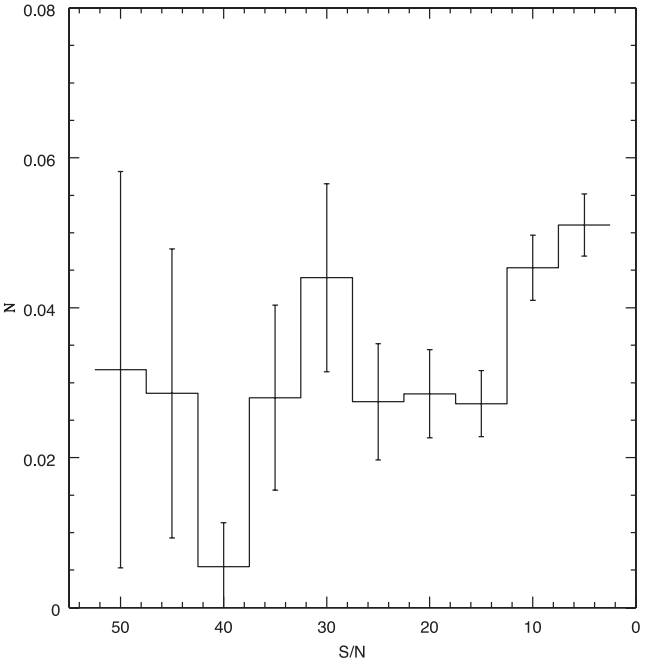

Figure 4. Fraction of detected magnetic DA white dwarfs versus S/N of the spectra.

The observed Zeeman splitting represents the mean field across the surface of the star. If the field is assumed as a dipole, the mean field is related to the polar field by

$$B = \frac{1}{2} B_{\rm p} \sqrt{1 + 3\cos^2\theta}\,,$$

where $B_{\rm p}$ is the polar field and θ is the angle between the field and the line of sight. Simple centred dipoles are rarely, if ever, seen in real stars (e.g. Külebi et al. 2009).

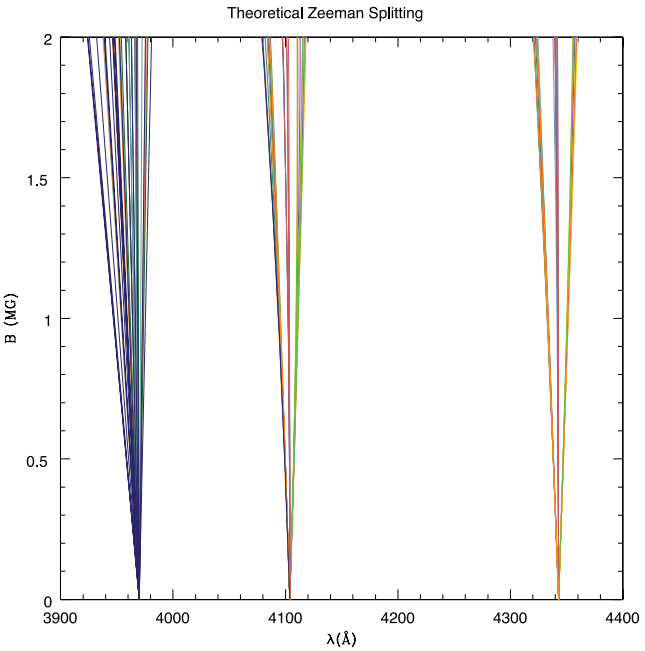

Figure 5. Hϵ, $n = 7 \rightarrow 2$, $\lambda_0 = 3971$ Å (left-hand side) to Hγ, $n = 5 \rightarrow 2$, $\lambda_0 = 4342$ Å (right-hand side) theoretical Zeemam splittings for $B = 0 \rightarrow 2$ MG, showing the higher lines split into multiplets even for these low fields, because the quadratic Zeeman splitting is proportional to n^4.

To estimate the magnetic fields, we measured the Hα and Hβ mean splittings independently and used the mean fields estimated by Külebi et al. (2009) as scale. Our measurements are of the mean line centres, by visual inspection, and therefore do not take into account the shape of the lines, which are different due to the fact that for most stars the magnetic field is not centred at the centre of the star (Külebi et al. 2009). Our estimates also ignore any effects due to higher moments than dipoles, or double-degenerate stars. The estimates are therefore very rough, but do indicate the order of magnitude of the magnetic field.

For fields above 30 MG, like for SDSS J085649.68+253441.07 shown in Fig. 6, line identification is difficult, and we adjusted graphically the spectra to the theoretical Zeeman positions only.

Fig. 7 shows fits of centred dipole magnetic models with $\log g = 8.0$ as those shown by Külebi et al. (2009) for five stars, to illustrate the discrepancies of assuming centred fields. Table 1 shows the estimated values for the magnetic fields for the 521 spectra we measured. The fifth column of the table shows the S/N in the region of the g filter of the spectra, S/N(g).

Fig. 8 shows the distribution of fields for our sample, showing an increase in the number of stars for lower fields, except for the lowest bin, where selection effects are important, as our $R \simeq 2000$ resolution implies we cannot detect $B \leq 2$ except at the highest S/N.

4 BLIND TEST

In order to check whether magnetic white dwarfs can be identified and analysed with sufficient confidence using noisy spectra, we have performed a blind test. One group has calculated model spectra for white dwarfs with and without magnetic fields for effective temperatures between 8000 and 40 000 K and $\log g = 8.0$. For the models with magnetic fields, we assumed centred magnetic dipoles with a polar field strength between 1 and 550 MG and viewing

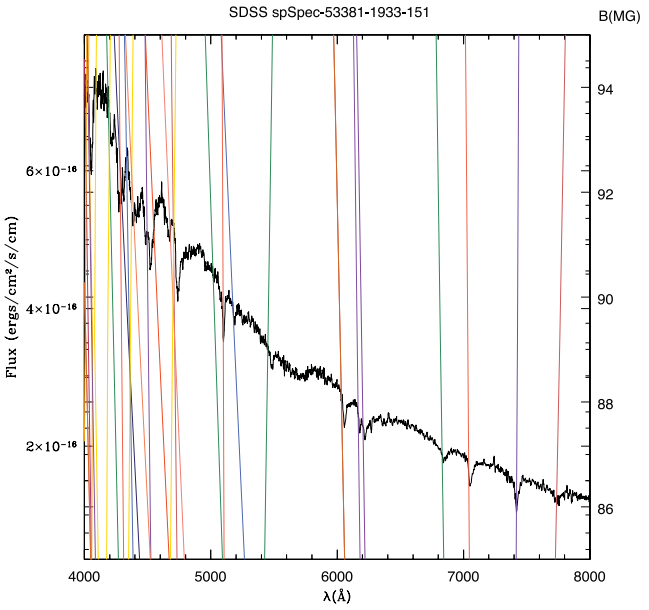

Figure 6. Spectrum for the SDSS J085649.68+253441.07 DA with a magnetic field around 90 MG, and the position of the theoretical Zeeman splittings (continuous coloured lines) for a dipole magnetic field B indicated on the right-hand side of the plot.

angles between the observer and the magnetic fields between 0° and 90°. Subsequently, we added Gaussian noise with S/N between 4 and 35.

In total 346 such spectra were given to the second group whose task was to identify which of the objects were magnetic and what the mean magnetic field strength was. This group did not know how many of the spectra were calculated assuming no magnetic fields and what the assumed field strengths for the magnetic objects were.

To be on the secure side, we assumed that all objects with a magnetic field lower than 2 MG were regarded as non-magnetic.

79 of the 346 noisy spectra were based on zero-field models (<2 MG). Only seven of them were wrongly classified as being magnetic and all of them had S/N below 8; in total, we have simulated 43 objects with S/N < 8. None of the false-detections had a determined field strength above 3 MG so that no non-magnetic white dwarf was regarded as having a strong magnetic field. If we disregard detections below 2 MG and S/N below 10, then we do not detect any false-magnetics.

41 of the noisy theoretical spectra were assigned to be non-magnetic by the second group but in fact had assumed magnetic fields larger than 2 MG. This number is indeed significantly large because we had in total 130 objects with simulated zero fields. At $B < 50$ MG, 13 out of 265 objects (5 per cent) were false-negatives. At $B > 50$ MG, we have 28 out of 81 objects (34 per cent false) false-negatives. The distribution between 50 and 400 MG is quite flat. If we limit ourselves to S/N above 10, the number of false-negatives is reduced to seven objects (out of 84) which all had relatively weak features (magnetic fields above 100 MG and effective temperature above 35 000 K). At S/N > 15 this number is further reduced to two objects (out of 52); at S/N > 20 (34 simulated objects) all simulated magnetic objects were determined as such.

The determined mean field strengths were compared to the mean magnetic fields of the dipole models. 214 of the theoretical spectra were calculated for field strengths between 1 and 100 MG. If we again limit ourselves to the ones with S/N above 10, the magnetic field determination 'by eye' was rather accurate. In only six cases, the determined magnetic field strength differed from the simulated one by more than a factor of 2.

At fields above 100 MG (53 simulated spectra), the magnetic field determination was less satisfactory even at S/N above 15. The magnetic fields were often wrong (mostly underestimated) by more than a factor of 2.

Without detailed modelling, the magnetic field determination at very high magnetic fields (>100 MG) is much more difficult than at lower fields. This is because most of the spectral lines are completely washed out by the quadratic Zeeman effect if the magnetic field varies over the stellar surface (this variation amounts to a factor of 2 in the case of dipole models). Only the so-called stationary line components for which the wavelengths go through maxima or minima as functions of the magnetic field strength remain visible. The corresponding field strength is not necessarily close to the mean field strength. This could partially explain the difference between the field determinations 'by eye' and the simulated values.

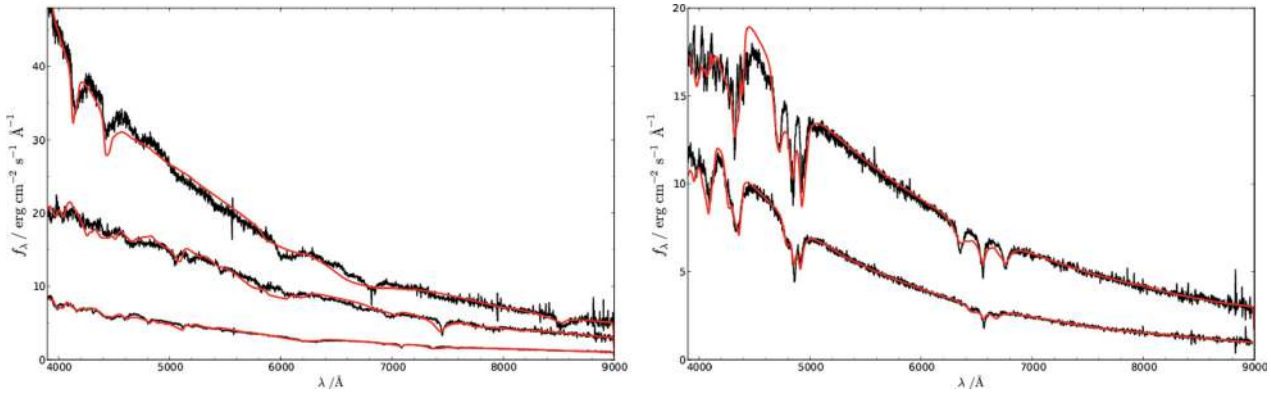

Figure 7. Sample fits done to five different objects using the method from Külebi et al. (2009), with the data base of centred dipolar models. The plots include the following observed spectra (black lines) with the best-fitting dipole models (red lines): (first part) SDSS J135141.13+541947.35 with (B_p = 500 MG), SDSS J021148.22+211548.19 (B_p = 168 MG), SDSS J101805.04+011123.52 (B_p = 127 MG); (second part) SDSS J125715.54+341439.38 (B_p = 12 MG), SDSS J074853.08+302543.56 (B_p = 6.8 MG). The fits are intended to be representative and the disagreements between the models and fits are due to a lack of detailed modelling in which the effective temperature and the sophisticated magnetic models have not been accounted for. In the plots, arbitrary factors of normalization have been used for display.

Table 1. Magnetic white dwarf stars. Notes: P-M-F denotes the Plate-Modified Julian Date-Fibre number which designates an SDSS spectrum. K in the Hβ magnetic field column means it was measured by Külebi et al. (2009). For those spectra we quote only their field determinations, as they fit the whole spectrum, keeping $\log g = 8.0$.*SDSS J125044.42+154957.3 is a $P_{\rm orb} = 86$ min binary (Breedt et al. 2012). The full table is available as online supporting information.

Name (SDSS J)	P-M-F	$B_{\rm H\alpha}$ (MG)	$B_{\rm H\beta}$ (MG)	S/N	g (mag)	$T_{\rm eff}$ (K)	σ_T (K)	$\log g$ (cgs)	σ_g (cgs)
135141.13+541947.35	1323-52797-293	773	K	37.71	16.40	10180	0084	09.64	0.26
234605.44+385337.69	1883-53271-272	706	K	17.74	18.89	99999	0794	05.00	0.01
100356.32+053825.59	0996-52641-295	668	K	15.28	18.11	14019	0140	09.98	0.03
120609.83+081323.72	1623-53089-573	312	K	09.34	19.03	10735	0247	07.65	0.38
221828.59−000012.21	0374-51791-583	212	K	17.30	18.13	12239	0443	09.73	0.24
021148.22+211548.19	2046-53327-048	105	K	36.09	16.73	12986	0134	09.99	0.06
085649.68+253441.07	1933-53381-151	90	–	28.44	17.51	10815	0200	09.91	0.10
080743.33+393829.18	0545-52202-009	65	K	04.07	20.14	10783	0418	08.93	0.67
170400.01+321328.66	0976-52413-319	56	K	04.07	20.42	25597	1118	09.39	0.21
023609.38−080823.91	0455-51909-474	54	–	06.47	19.75	08733	0145	09.93	0.08
114006.37+611008.21	0776-52319-042	53	K	06.41	19.67	10540	0326	09.45	0.45
224741.46+145638.76	0740-52263-444	47	K	29.37	17.39	14771	0069	10.00	0.01
214930.74−072811.97	0644-52173-350	45	K	31.93	17.41	72000	1337	10.00	0.01
121635.36−002656.22	0288-52000-276	45	K	06.51	19.58	11150	0286	09.70	0.26
160357.93+140929.97	2524-54568-247	43	–	16.91	18.29	10123	0055	09.26	0.44
101805.04+011123.52	0503-51999-244	40	K	49.54	16.31	10108	0043	09.87	0.11
094235.02+205208.32	2292-53713-019	38	K	14.39	18.44	13277	0140	09.99	0.02
160437.36+490809.18	0622-52054-330	38	K	20.94	17.90	10084	0012	09.25	0.60
125416.01+561204.67	1318-52781-299	37	K	08.59	19.01	10338	0172	08.62	0.53
151415.66+074446.50	1817-53851-534	36	K	14.92	18.84	10090	0024	09.55	0.38
082835.82+293448.69	1207-52672-635	35	K	06.17	19.74	13176	0327	09.88	0.13
114828.99+482731.23	1446-53080-324	33	K	17.05	18.16	89520	5406	10.00	0.01
075819.57+354443.70	0757-52238-144	32	K	22.10	18.20	12930	0100	10.00	0.01
080938.10+373053.81	0758-52253-044	31	K	10.33	19.01	11398	0320	09.56	0.29
142703.35+372110.51	1381-53089-182	30	34	23.95	17.55	49950	0990	10.00	0.01
172329.14+540755.82	0359-51821-415	30	K	10.13	18.80	10157	0092	09.15	0.50
085153.79+152724.94	2431-53818-238	29	32	08.38	19.42	11300	0388	09.58	0.31
080440.35+182731.03	2081-53357-442	29	K	18.23	18.11	10135	0063	08.46	0.39
011423.35+160727.51	2825-54439-548	28	29	16.90	19.50	46537	1332	10.00	0.01
080359.94+122944.02	2265-53674-033	27	K	31.03	17.27	12347	0109	09.99	0.02
172932.48+563204.09	0358-51818-239	27	K	05.56	20.03	10277	0182	09.18	0.62
115418.14+011711.41	0515-52051-126	26	K	19.69	17.75	79747	3659	10.00	0.01
093415.97+294500.43	2914-54533-162	25	32	25.07	18.95	61840	1821	10.00	0.01
122401.48+415551.91	1452-53112-181	25	K	12.32	18.94	10100	0034	09.35	0.46
113839.51−014903.00	0327-52294-583	24	K	28.51	17.61	10198	0095	09.47	0.31
215148.31+125525.49	0733-52207-522	22	K	20.11	18.10	43262	1151	09.99	0.02
232248.22+003900.88	0383-51818-421	22	K	08.90	19.12	13458	0190	09.97	0.04
023420.63+264801.71	2399-53764-559	21	K	28.75	18.39	57403	0981	10.00	0.01
105628.49+652313.45	0490-51929-205	21	K	09.28	19.71	43262	1894	09.99	0.02
125553.39+152555.08	1771-53498-343	20	2	06.74	19.52	15263	0536	07.68	0.16
125044.43+154957.36*	1770-53171-530	20	K	16.23	18.28	10082	0010	09.66	0.35
125715.54+341439.38	2006-53476-332	19	19	36.15	16.80	38124	0288	10.00	0.01
091124.68+420255.85	1200-52668-538	19	K	13.77	18.84	10108	0043	09.51	0.36
120150.13+614256.93	0778-54525-280	19	17	14.68	18.48	08122	0076	10.00	0.01
	0778-52337-264	8	K	13.50					
105404.38+593333.34	0561-52295-008	18	K	03.51	20.27	09313	0382	09.93	0.08
084201.42+153941.89	2429-53799-363	17	17	06.90	19.73	22510	0794	10.00	0.01
032628.17+052136.35	2339-53729-515	17	K	17.94	18.95	55082	1926	09.99	0.01
225726.05+075541.71	2310-53710-420	17	K	34.35	17.10	85279	2742	09.99	0.02
094458.92+453901.15	1202-52672-577	17	K	05.79	19.92	18919	1136	10.00	0.01
122209.43+001534.06	2568-54153-471	16	K	08.33	20.26	21070	0749	10.00	0.01
	0289-51990-349	16	K	03.23					
053317.32−004321.91	2072-53430-096	16	11	17.06	00.00	71388	5460	07.10	0.24
153829.29+530604.65	0795-52378-637	16	K	08.51	19.26	18116	0547	10.00	0.01
131508.97+093713.87	1798-53851-233	14	–	45.27	16.23	72414	1249	10.00	0.01
074924.91+171355.45	2729-54419-282	14	K	22.57	18.78	35795	0432	10.00	0.01
072540.82+321402.12	2695-54409-564	14	13	07.43	20.06	34711	1100	09.99	0.02
100759.81+162349.64	2585-54097-030	14	K	22.19	17.74	32642	0275	10.00	0.01
083448.65+821059.00	2549-54523-135	14	K	28.14	18.33	41210	0539	10.00	0.01
134820.80+381017.25	2014-53460-236	14	K	23.58	17.55	45528	0864	10.00	0.01
133340.34+640627.38	0603-52056-112	14	K	19.01	17.88	20048	0152	10.00	0.01

Table 1 – *continued*

Name (SDSS J)	P-M-F	$B_{H\alpha}$ (MG)	$B_{H\beta}$ (MG)	S/N	g (mag)	$T_{\rm eff}$ (K)	σ_T (K)	$\log g$ (cgs)	σ_g (cgs)
115345.97+133106.61	1762-53415-042	13	–	05.56	19.81	12844	0540	09.19	0.40
143235.46+454852.52	2932-54595-542	13	K	09.68	19.94	21053	0492	09.99	0.02
101428.10+365724.40	1954-53357-393	13	13	12.95	18.85	19580	0342	10.00	0.01
140716.67+495613.70	1671-53446-453	13	K	09.49	19.14	27376	0610	10.00	0.01
101428.10+365724.40	1426-52993-021	13	13	08.49	18.85	17225	0724	09.99	0.02
205233.52−001610.69	0982-52466-019	13	K	12.40	18.51	36761	0831	09.99	0.01
074947.00+354055.51	0542-51993-639	13	12	11.00	19.75	39100	1213	09.98	0.03
152401.60+185659.21	2794-54537-410	12	K	20.77	18.16	22067	0290	10.00	0.01
085550.68+824905.20	2549-54523-066	12	K	22.40	18.64	32081	0265	10.00	0.01
103350.88+204729.40	2376-53770-463	12	13	08.00	19.42	34544	0947	09.98	0.03
090748.82+353821.5	1212-52703-187	12	K	–	19.61	12485	0306	09.85	0.14
001034.95+245131.20	2822-54389-025	11	11	10.43	19.84	19355	0654	10.00	0.01
075234.95+172524.86	2729-54419-171	11	11	28.79	18.46	39779	0471	10.00	0.01
	1920-53314-106	12	K	17.67					
202501.11+131025.62	2257-53612-167	11	K	23.72	18.77	28932	0199	10.00	0.01
120547.48+340811.48	2089-53498-431	11	12	09.00	19.63	23237	0632	10.00	0.01
033145.69+004517.04	0810-52672-391	11	11	45.85	17.20	28299	0095	10.00	0.01
	2049-53350-450	11	11	33.80					
	0415-51879-378	12	13	32.22					
	0415-51810-370	12	K	32.86					
081648.71+041223.53	1184-52641-329	11	10	03.44	20.39	12880	0912	09.95	0.06
030407.40−002541.74	0709-52205-120	11	11	26.97	17.75	21828	0227	10.00	0.01
	2048-53378-280	10	10	26.18					
	0411-51817-172	11	10	23.40					
	0411-51873-172	19	18	22.83					
	0710-52203-311	11	11	21.25					
115917.39+613914.32	0777-52320-069	10	K	07.64	18.97	35770	1193	09.99	0.02
121209.31+013627.72	0518-52282-285	10	K	21.90	18.00	24706	0182	10.00	0.01
031824.20+422651.00	2417-53766-568	9.9	9.2	30.87	18.21	20274	0098	10.00	0.01
084008.50+271242.70	1587-52964-059	9.8	10	08.06	19.17	19113	0355	09.99	0.02
172045.37+561214.90	0367-51997-461	9.7	K	06.24	20.10	46580	3487	09.95	0.06
153843.11+084238.27	1725-54266-297	9.6	K	19.58	17.92	33803	0340	09.99	0.01
165203.68+352815.81	0820-52438-299	9.5	K	09.99	19.23	18778	0406	09.94	0.07
034308.18−064127.35	0462-51909-117	9.2	K	08.82	19.48	11718	0447	09.57	0.32
153532.25+421305.62	1052-52466-252	9.1	K	03.21	20.37	18143	1006	08.10	0.24
091437.35+054453.31	1193-52652-481	8.9	K	28.18	17.33	23420	0229	10.00	0.01
123204.20+522548.27	0885-52379-319	8.9	9.6	10.25	18.82	08183	0093	09.29	0.10
124851.31−022924.73	2922-54612-607	8.8	8.7	34.75	18.42	19835	0070	10.00	0.01
112030.34-115051.14	2874-54561-512	8.8	8.7	21.88	18.73	27302	0222	10.00	0.01
093126.14+321946.15	1943-53386-294	8.6	8.3	07.49	19.23	16248	0629	09.58	0.12
122249.14+481133.14	1451-53117-582	8.6	8.3	13.72	18.72	09790	0093	10.00	0.01
151130.17+422023.00	1291-52735-612	8.4	K	19.79	17.99	30882	0265	10.00	0.01
	1291-52738-615	12	12	18.41					
154213.48+034800.43	0594-52045-400	8.2	K	11.35	19.12	15760	0877	10.00	0.01
113756.50+574022.43	1311-52765-421	8.1	8.3	29.48	16.87	10080	0002	09.03	0.80

We conclude that we can distinguish between spectra from magnetic (>2 MG) and non-magnetic white dwarfs (≤2 MG) with very high confidence if we limit ourselves to spectra with S/N above 10. Hot magnetic white dwarfs with effective temperatures above 35 000 K and fields above 100 MG can be missed due to their shallow features. For field strength above 100 MG we generally have to assume large uncertainties in the 'by eye' field determination.

5 VARIABLE FIELDS

For 11 stars we have from two to six independent co-added spectra, obtained at different epochs, and for a few of them we could see significant changes in the Zeeman splittings, probably due to an inclined magnetic field axis with respect to the rotational axis of the star. For SDSS J030407−002541.74, for example, shown in Fig. 9, the structure of the Zeeman splitting changes substantially, indicating either a very complex magnetic structure or possibly a double-degenerate magnetic system. We do not have time-series spectra to study their variability time-scale, but such changes in the line profiles have been detected for other magnetic white dwarfs, due to rotation (e.g. Burleigh, Jordan & Schweizer 1999; Euchner et al. 2002, 2005, 2006). Breedt et al. (2012) show that some of the magnetic white dwarfs are in fact white dwarf binaries, when phase-resolved spectra are obtained.

6 THE EFFECT OF MAGNETIC FIELD ON MASS ESTIMATES

The mass distribution of the hydrogen-rich DAs shows an effect, which is well documented since many years, but still not fully

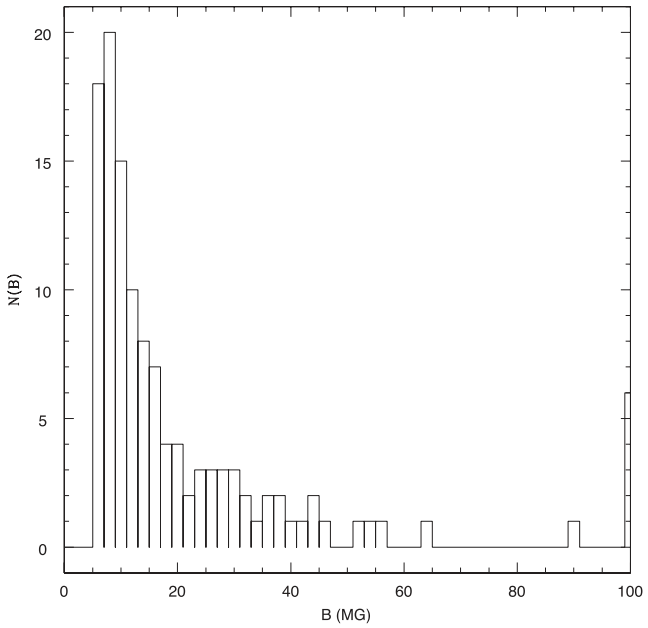

Figure 8. Number of white dwarfs versus magnetic field for the SDSS sample. As our detection limit is around 1–2 MG, selection effects in the lowest bin are important.

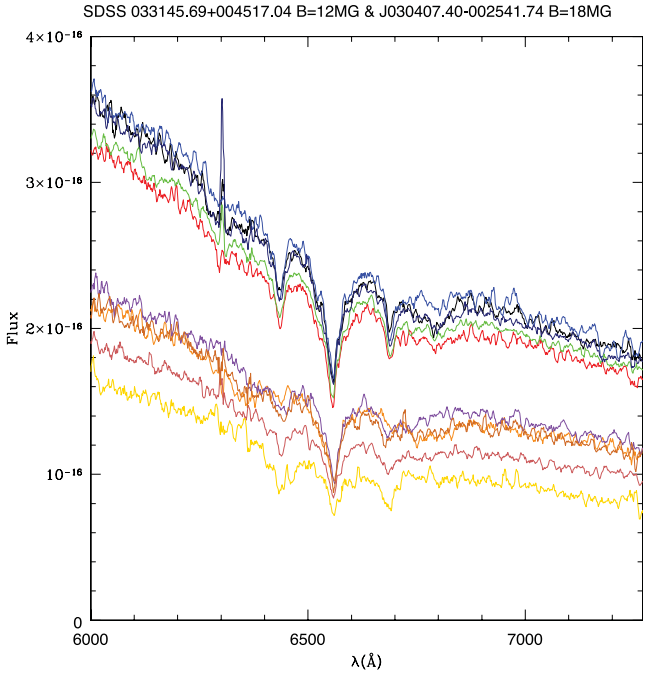

Figure 9. Spectra for different epochs for SDSS J033145.69+004517, with $B = 12$ MG (top), and SDSS J030407.40−002541.74, with $B = 18$ MG (bottom). The last star set of spectra show significant changes in the Zeeman splittings with time. The spectra are purposefully not offset from each other.

understood: the average mass, as estimated by the surface gravity, increases apparently below 13 000 K for DAs (Bergeron, Saffer & Liebert 1991; Koester 1991; Kleinman et al. 2004; Liebert, Bergeron & Holberg 2005; Kepler et al. 2007; Gianninas et al. 2010; Limoges & Bergeron 2010; Gianninas, Bergeron & Ruiz 2011; Tremblay, Bergeron & Gianninas 2011a). Single white dwarf masses in these studies are typically determined through spectroscopy – measuring

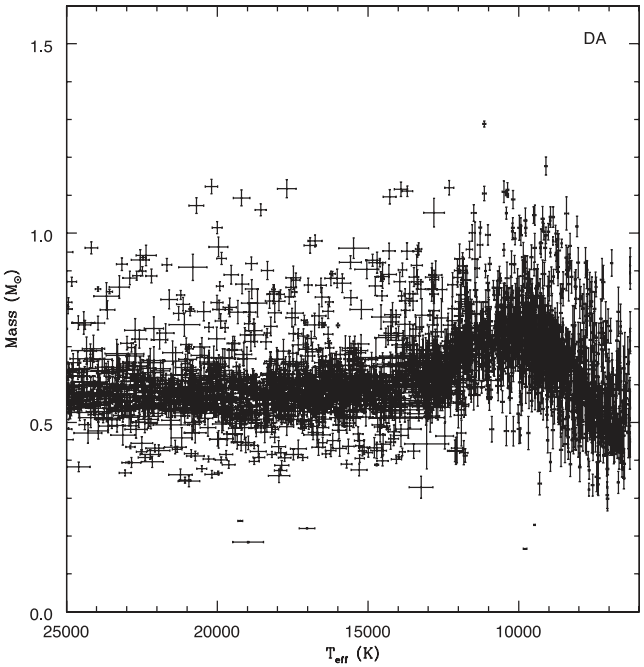

Figure 10. Masses for DA stars measured from the S/N ≥ 15 SDSS optical spectra by Kleinman et al. (2013), showing the apparent increase in the derived masses around $T_{\rm eff} \leq 13\,000$ K, which are not seen in the masses derived by colours or gravitational redshift.

linewidths due to Stark and neutral pressure broadening. Mass determinations from photometry and gravitational redshift (Engelbrecht & Koester 2007; Falcon et al. 2010) do not show this mass increase, so the increase is probably not real, and merely reflects some failure of the input physics in our spectroscopic models. Efforts have been made to improve the treatment of the line broadening (Koester et al. 2009a; Tremblay et al. 2010), but the apparent mass increase remains (Gianninas et al. 2010, 2011; Tremblay et al. 2011a). In Fig. 10, we show the masses for DAs with S/N ≥ 15 spectra in Kleinman et al. (2013).

Other proposed explanations for the broadening were the treatment of the hydrogen-level occupation probability, or convection bringing up subsurface He to the atmosphere, increasing the local pressure. However, no evidence for the He could be found, leaving the very description of convection with the usual mixing length approximation as the most likely culprit (Koester et al. 2009a; Tremblay et al. 2010). Calculations using realistic 3D simulations of convection seem to confirm this assumption (Tremblay et al. 2011b).

In this study, we explore a complementary possibility for the broadening of the spectral lines below $T_{\rm eff} \simeq 13\,000$ K, the presence of weak magnetic fields in the cooler white dwarfs. Unresolved Zeeman splitting can increase the apparent linewidths and mimic a stronger Stark broadening, especially for the higher lines. Since the spectroscopic gravity determination is based on the linewidths, an average mass white dwarf star with a weak magnetic field can appear spectroscopically indistinguishable from a non-magnetic, massive star. The combined effect of electric and magnetic fields on the spectral lines is very complicated and has been studied only for special cases of the geometry (e.g. Friedrich et al. 1994; Külebi et al. 2009). Detailed model grids, which include also the effect of the magnetic field on the radiative transfer, are therefore not yet available. We find an increase in the mean field around the same temperature when these stars develop a surface convection zone,

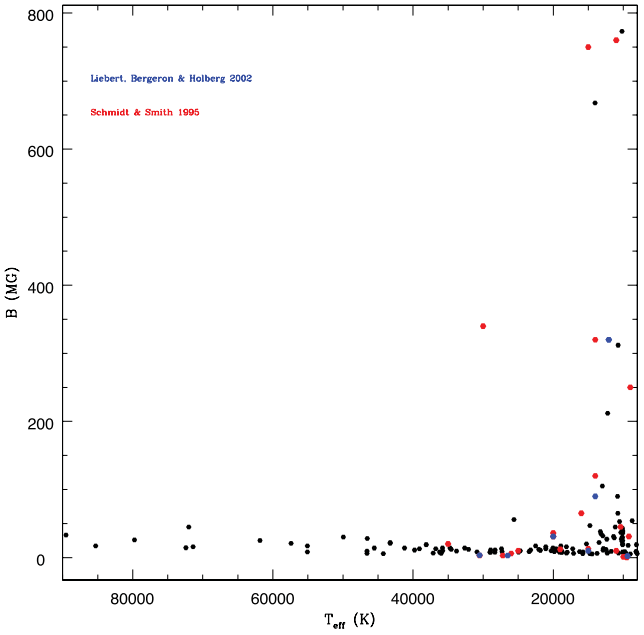

Figure 11. Magnetic field versus effective temperature for the SDSS sample, Liebert et al. (2003) and Schmidt & Smith (1995), showing an increase in field for $T_{\rm eff} \leq 13\,000$ K, where a surface convection zone develops. As the number of stars is larger at lower temperatures, just because they cool on a longer time-scale, the fraction of higher field stars is an important parameter.

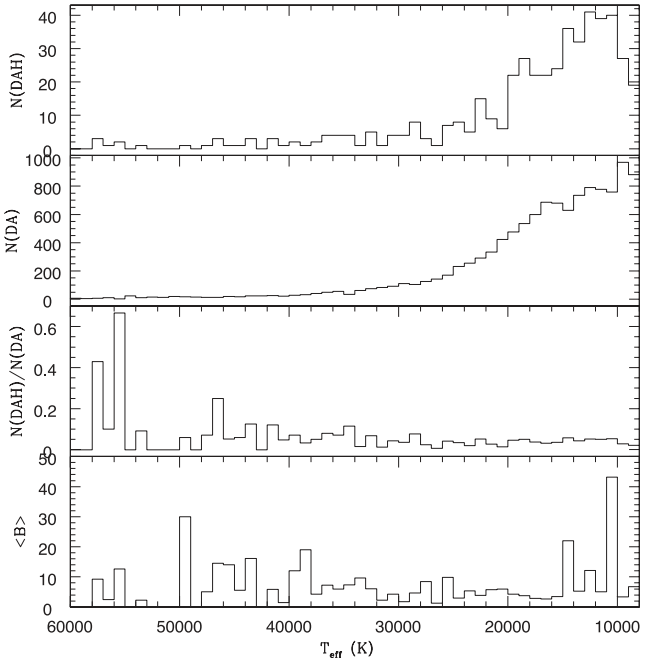

Figure 12. The top two panels show the number of DAHs and DAs versus $T_{\rm eff}$. The third panel from the top shows the ratio of the number of DAHs to the number of DAs. In the lowest panel, we see the mean field for DAHs of that $T_{\rm eff}$, showing that even though the fraction of magnetic to non-magnetic field measured with $B > 2$ MG does not increase at lower $T_{\rm eff}$, the mean field does increase.

raising the possibility that the surface convection zone is amplifying an underlying magnetic field (Figs 11 and 12).

As the Zeeman splitting broadens the lines, we cannot use the line profiles to estimate their surface gravity directly. For fields stronger than $B \simeq 1$ MG, the magnetic splittings for the $n = 7$–10 energy levels of hydrogen wash out the lines, just like high gravity does. As shown in Fig. 5, the theoretical Zeeman splittings for the Balmer lines initiate at $n = 7$ (Hϵ, $\lambda_0 = 3971$ Å) to $n = 5$ (Hγ), showing the higher lines split into multiplets even for fields below $B = 1$ MG. Unfortunately, there are no published calculations of the splittings for hydrogen levels higher than $n = 7$ for these fields, where perturbation theory is no longer applicable (Jordan 1992; Ruder et al. 1994). For these higher levels, the Zeeman splitting calculations need higher order terms even for fields of the order of 1 MG.

As we detected Zeeman splitting in the disc integrated spectra for 4 per cent or more of white dwarfs, which comes from global organized fields, perhaps even smaller or unorganized fields are the cause for the line broadening on these cooler stars.

It will be necessary to investigate if surface convection amplification of an underlying weak magnetic field is causing broadening of the spectral lines of white dwarf stars cooler than 13 000 K, leading to misinterpretation of these stars as more massive stars.

Even weaker magnetic fields in white dwarfs have been studied by Koester et al. (1998), who obtained high-resolution spectrum measurements of the non-local thermodynamic equilibrium core of Hα for 28 white dwarf stars to measure their projected rotational velocities, finding three magnetic white dwarfs, and no fields above 10–20 kG for the other stars, all hotter than 14 000 K. Koester et al. (2009b) observed about 800 white dwarfs in the SPY survey, finding 10 as magnetic, with fields from 3 to 700 kG. Kawka & Vennes (2012) studied 58 white dwarfs with ESO/VLT/FORS1 spectropolarimetry and estimated 5 per cent of white dwarfs with fields from 10 to 100 kG. Landstreet et al. (2012) estimate that 10 per cent of all white dwarf stars have kG fields from ESO/VLT/FORS spectropolarimetry.

7 MEAN MASSES

Wickramasinghe & Ferrario (2005) quote a mean mass of 0.93 $M_\odot$ for magnetic white dwarfs, based on Liebert et al. (2003) determinations, but the sample includes only a handful of stars with astrometric measured masses, so the evidence that the magnetic white dwarfs are more massive than the average was scarce. Kawka et al. (2007) obtained a mean mass of 0.78 $M_\odot$ for the 28 magnetic DA white dwarfs with mass estimates, mainly from fitting the line wings of the spectra.

We estimated the masses for every star with S/N(g) ≥ 10 spectra, from their u, g, r, i, z colours, shown in Fig. 13, obtaining for the 84 hydrogen-rich magnetic white dwarfs (DAHs) with $B \leq 3$ MG $\langle M \rangle = (0.68 \pm 0.04)\,M_\odot$. For the 71 DAHs with $B > 3$ MG, $\langle M \rangle = (0.83 \pm 0.04)\,M_\odot$. Fig. 14 shows the mass histogram for stars with fields lower and higher than $B = 3$ MG, compared to non-magnetic ones, demonstrating that there is an increase in the estimated mass for magnetic stars, but the estimated mass values are uncertain because the u colour is severely affected by magnetic fields, caused by the n^4 dependency of the splittings (e.g. Girven et al. 2010). The estimated masses are much larger than the mean masses for the 1505 bright and hot DA white dwarfs in Kleinman et al. (2013), that is, those with S/N ≥ 15 and $T_{\rm eff} \geq 13\,000$ K, for which we did not detect any magnetic field, $\langle M \rangle_{\rm DA} = (0.593 \pm 0.002)\,M_\odot$. Even though we find a higher mass for DAHs, our mean is much smaller than the mean masses quoted for the few previously measured magnetic DAs.

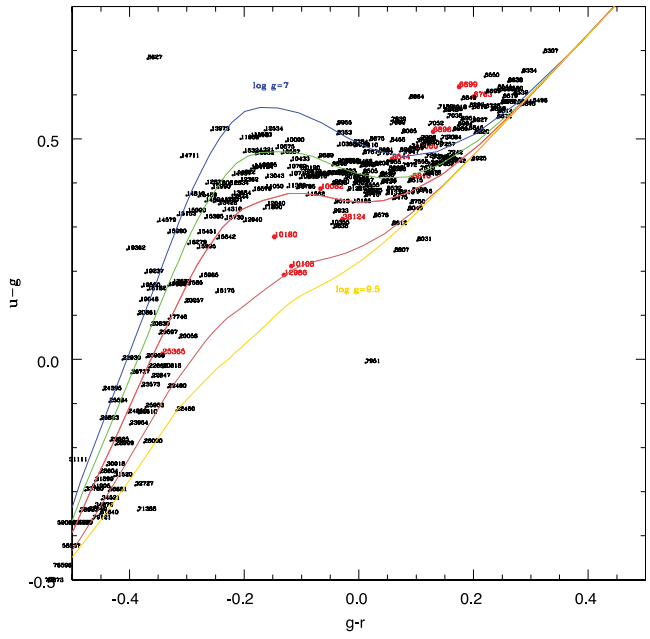

Figure 13. Colours for normal DAs (black) and DAHs (red), showing both follow the characteristic curves, but with an excess of DAHs (red) for higher log g. We again caution the reader that the log g estimates are very uncertain for the magnetic stars because the u colour, where the Balmer jump is located, is heavily affected by the magnetic field.

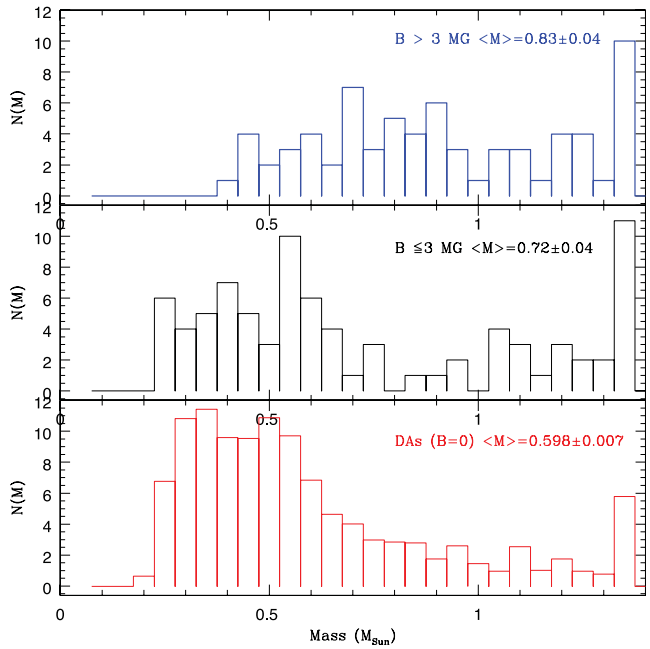

Figure 14. Mass histogram from colours for low-field (black) and high-field (blue) DAHs and DAs, showing the apparent masses increase with increasing magnetic field.

8 DISCUSSION

Considering only spectra with S/N $\geq$ 10, we increased the number of known magnetic DAs by a factor of 2. We estimated the field strength for 521 stars. Our blind test shows we underestimate the number of magnetics in the simulation and underestimate the field in general. Even for S/N $\leq$ 10, our candidates have at least a 50 per cent chance of being magnetic, compared to only 4 per cent in field white dwarfs. We showed that the magnetic field changes with time for a few stars for which we have multiple spectra, that stars with surface temperatures where the convection zone develops seem to show stronger magnetic fields than hotter stars, and that the mean mass of magnetic stars seems to be on average larger than the mean mass of non-magnetic stars.

If the apparent increase in masses shown in Fig. 10 were only caused by magnetic field amplification when the surface convection zone appears around $T_{\rm eff} \leq 13\,000$ K, it should, perhaps, continue to rise at lower temperatures. However, if the mass of the convection zone becomes high enough that its kinetic energy is of the same order as the magnetic energy, amplification will not be effective.

Zorotovic, Schreiber & Gänsicke (2011) estimate the mean white dwarf mass among cataclysmic variables (CVs) is $\langle M_{\rm CV}\rangle = (0.83 \pm 0.23)\,{\rm M}_{\odot}$, much larger than that found for pre-CVs, $\langle M_{\rm PCV}\rangle = (0.67 \pm 0.21)\,{\rm M}_{\odot}$, and single white dwarfs. Are all the magnetic white dwarfs descendants of binaries?

The *Gaia* mission will provide parallaxes for all these objects and thereby obtain strong constraints on magnetic and convection models and get an independent check of the surface gravity (log g) determinations, if we assume a mass–radius relation.

ACKNOWLEDGMENTS

SOK, JESC, IP and VP are supported by CNPq and FAPERGS – Pronex – Brazil. BGC is supported by the Austrian Fonds zur Förderung der wissenschaftlichen Forschung through project P 21830-N16. BK is supported by the MICINN grant AYA08-1839/ESP, ESF EUROCORES Program EuroGENESIS (MICINN grant EUI2009-04170), 2009SGR315 of the Generalitat de Catalunya and EU-FEDER funds. DEW gratefully acknowledges the support of the US National Science Foundation under grant AST-0909107 and the Norman Hackerman Advanced Research Program under grant 003658-0252-2009. AK is supported by CNPq. Funding for the SDSS and SDSS-II was provided by the Alfred P. Sloan Foundation, the Participating Institutions, National Science Foundation, US Department of Energy, National Aeronautics and Space Administration, Japanese Monbukagakusho, Max Planck Society and Higher Education Funding Council for England. The SDSS website is http://www.sdss.org/. The SDSS is managed by the Astrophysical Research Consortium for the Participating Institutions. The Participating Institutions are the American Museum of Natural History, Astrophysical Institute Potsdam, University of Basel, University of Cambridge, Case Western Reserve University, University of Chicago, Drexel University, Fermilab, Institute for Advanced Study, Japan Participation Group, The Johns Hopkins University, Joint Institute for Nuclear Astrophysics, Kavli Institute for Particle Astrophysics and Cosmology, Korean Scientist Group, Chinese Academy of Sciences (LAMOST), Los Alamos National Laboratory, Max Planck Institute for Astronomy (MPIA), Max Planck Institute for Astrophysics (MPA), New Mexico State University, Ohio State University, University of Pittsburgh, University of Portsmouth, Princeton University, United States Naval Observatory and University of Washington.

REFERENCES

Babcock H. W., 1947a, PASP, 59, 112
Babcock H. W., 1947b, ApJ, 105, 105
Bergeron P., Saffer R. A., Liebert J., 1991, in Vauclair G., Sion E., eds, White Dwarfs. Kluwer, Dordrecht, p. 75

Braithwaite J., Spruit H. C., 2004, Nat, 431, 839
Breedt E., Gänsicke B. T., Girven J., Drake A. J., Copperwheat C. M., Parsons S. G., Marsh T. R., 2012, MNRAS, 423, 1437
Burleigh M. R., Jordan S., Schweizer W., 1999, ApJ, 510, L37
Das U., Mukhopadhyay B., 2012, IJMPD, 21, 11, 1242001
Engelbrecht A., Koester D., 2007, in Napiwotzki R., Burleigh M. R., eds, ASP Conf. Ser. Vol. 372, White Dwarfs. Astron. Soc. Pac., San Francisco, p. 289
Euchner F., Jordan S., Beuermann K., Gänsicke B. T., Hessman F. V., 2002, A&A, 390, 633
Euchner F., Reinsch K., Jordan S., Beuermann K., Gänsicke B. T., 2005, A&A, 442, 651
Euchner F., Jordan S., Beuermann K., Reinsch K., Gänsicke B. T., 2006, A&A, 451, 671
Falcon R. E., Winget D. E., Montgomery M. H., Williams K. A., 2010, ApJ, 712, 585
Friedrich S., Ostreicher R., Ruder H., Zeller G., 1994, A&A, 282, 179
García-Berro E. et al., 2012, ApJ, 749, 25
Garstang R. H., 1977, Rep. Prog. Phys., 40, 105
Giammichele N., Bergeron P., Dufour P., 2012, ApJS, 199, 29
Gianninas A., Bergeron P., Dupuis J., Ruiz M. T., 2010, ApJ, 720, 581
Gianninas A., Bergeron P., Ruiz M. T., 2011, ApJ, 743, 138
Girven J., Gänsicke B. T., Külebi B., Steeghs D., Jordan S., Marsh T. R., Koester D., 2010, MNRAS, 404, 159
Greenstein J. L., Henry R. J. W., O'Connell R. F., 1985, ApJ, 289, L25
Hamada T., 1971, PASJ, 23, 271
Holberg J. B., Sion E. M., Oswalt T. D., 2011, BAAS, 43, #341.02
Jenkins F. A., Segrè E., 1939, Phys. Rev., 55, 52
Jordan S., 1992, A&A, 265, 570
Jordan S., Aznar Cuadrado R., Napiwotzki R., Schmid H. M., Solanki S. K., 2007, A&A, 462, 1097
Kawka A., Vennes S., 2012, MNRAS, 425, 1394
Kawka A., Vennes S., Wickramasinghe D. T., Schmidt G. D., Koch R., 2003, in de Matino D., Silvotti R., Solheim J.-E., Kalytis R., eds, White Dwarfs. Kluwer, Dordrecht, p. 179
Kawka A., Vennes S., Schmidt G. D., Wickramasinghe D. T., Koch R., 2007, ApJ, 654, 499
Kemp J. C., 1970, ApJ, 162, L69
Kepler S. O., Kleinman S. J., Nitta A., Koester D., Castanheira B. G., Giovannini O., Costa A. F. M., Althaus L., 2007, MNRAS, 375, 1315
Kleinman S. J. et al., 2004, ApJ, 607, 426
Kleinman S. J. et al., 2013, ApJS, 204, 5
Koester D., 1991, in Vauclair G., Sion E. M., eds, White Dwarfs. Kluwer, Dordrecht, p. 343
Koester D., 2010, Mem. Soc. Astron. Ital., 81, 921
Koester D., Dreizler S., Weidemann V., Allard N. F., 1998, A&A, 338, 612
Koester D., Kepler S. O., Kleinman S. J., Nitta A., 2009a, J. Phys.: Conf. Ser., 172, 012006
Koester D., Voss B., Napiwotzki R., Christlieb N., Homeier D., Lisker T., Reimers D., Heber U., 2009b, A&A, 505, 441
Külebi B., Jordan S., Euchner F., Gänsicke B. T., Hirsch H., 2009, A&A, 506, 1341
Kundu A., Mukhopadhyay B., 2012, MPLA, 27, 15, 1250084-1
Landstreet J. D., Bagnulo S., Valyavin G. G., Fossati L., Jordan S., Monin D., Wade G., 2012, A&A, 545, 30
Liebert J., Fleming T. A., Green R. F., Grauer A. D., 1988, PASP, 100, 187
Liebert J., Bergeron P., Holberg J. B., 2003, AJ, 125, 348
Liebert J., Bergeron P., Holberg J. B., 2005, ApJS, 156, 47
Limoges M.-M., Bergeron P., 2010, ApJ, 714, 1037
Nordhaus J., 2011, Int. J. Mod. Phys. E, 20, 29
Power J., Wade G. A., Aurière M., Silvester J., Hanes D., 2008, Constrib. Astron. Obs. Skalnaté Pleso, 38, 443
Roesner W., Wunner G., Herold H., Ruder H., 1984, J. Phys. B – At. Mol. Phys., 17, 29
Ruder H., Wunner G., Herold H., Geyer F., 1994, Atoms in Strong Magnetic Fields. Quantum Mechanical Treatment and Applications in Astrophysics and Quantum Chaos. Springer-Verlag, Heidelberg
Schmidt G. D., Smith P. S., 1995, ApJ, 448, 305
Sion E. M., Fritz M. L., McMullin J. P., Lallo M. D., 1988, AJ, 96, 251
Tout C.-A., Regos B., 1995, in Buckley D. A. H., Warner B., eds, ASP Conf. Ser. Vol. 85, Cape Workshop on Magnetic Cataclysmic Variables. Astron. Soc. Pac., San Francisco, p. 477
Tout C. A., Wickramasinghe D. T., Ferrario L., 2004, MNRAS, 355, L13
Tout C. A., Wickramasinghe D. T., Liebert J., Ferrario L., Pringle J. E., 2008, MNRAS, 387, 897
Tremblay P.-E., Bergeron P., Kalirai J. S., Gianninas A., 2010, ApJ, 712, 1345
Tremblay P.-E., Bergeron P., Gianninas A., 2011a, ApJ, 730, 128
Tremblay P.-E., Ludwig H.-G., Steffen M., Bergeron P., Freytag B., 2011b, A&A, 531, L19
Wegg C., Phinney E. S., 2012, MNRAS, 426, 427
Wickramasinghe D. T., Ferrario L., 1988, ApJ, 327, 222
Wickramasinghe D. T., Ferrario L., 2005, MNRAS, 356, 1576
Zorotovic M., Schreiber M. R., Gänsicke B. T., 2011, A&A, 536, A42

SUPPORTING INFORMATION

Additional Supporting Information may be found in the online version of this article:

Table 1. Magnetic white dwarf stars. (http://mnras.oxfordjournals.org/lookup/suppl/doi:10.1093/mnras/sts522/-/DC1).

Please note: Oxford University Press are not responsible for the content or functionality of any supporting materials supplied by the authors. Any queries (other than missing material) should be directed to the corresponding author for the article.

This paper has been typeset from a TEX/LATEX file prepared by the author.